NANO LETTERS

2007
Vol. 7, No. 5
1439−1443

Electron Dephasing and Weak Localization in Sn Doped In_2O_3 Nanowires

Adenilson J. Chiquito,*,† Alexandre J. C. Lanfredi,‡ Rafaela F. M. de Oliveira,† Livia P. Pozzi,† and Edson R. Leite‡

Departamento de Física, Universidade Federal de São Carlos, CEP 13565-905, CP 676 São Carlos, São Paulo, Brazil, and Laboratório Interdisciplinar de Eletroquímica e Cerâmicas, Departamento de Química, Universidade Federal de São Carlos, CEP 13565-905, CP 676 São Carlos, São Paulo, Brazil

Received January 23, 2007; Revised Manuscript Received March 23, 2007

ABSTRACT

We report on (magneto-) transport measurements of individual In_2O_3 nanowires. We observed that the presence of a weak disorder arising from doping and electron−boundary collisions leads to weak localization of electrons as revealed by the positive magnetoconductivity in a large range of temperatures (∼77 K). From temperature-dependent resistance and magnetoconductivity data, the electron−electron interaction was pointed out as the mechanism responsible for the increase of resistance in the low temperature range and the dominant source of the dephasing at low temperatures. The experimental data provided the phase coherence time $\tau_\phi \sim T^{-2/3}$ expected for 1D systems, giving consistent support to the mechanisms underlying the weak-localization and electron−electron scattering theories.

The potential electronic applications of Sn doped In_2O_3 (ITO) nanowires requires a detailed understanding of their fundamental electronic properties. Great effort has been devoted on developing semiconducting nanowires and carbon nanotubes due to their characteristic features for application in devices and in nanoelectronics.[1−4] Its nanoscale dimension makes them also interesting from the point of view of fundamental physics because they are structures where the quantum mechanical interactions cannot be neglected. For instance, conventional mechanisms of current transport such as ohmic conduction are no longer valid in the quantum transport regime, which in turn, is believed as the dominant regime in that structures.[5−7] Quantum coherence of electrons in condensed matter remains a very attractive topic because the coherent control of electrons and the study of decoherence mechanisms (and their dependence on the temperature) are fundamental for novel devices such as those built using ITO nanowires. In fact, the study of dephasing mechanisms in nanostructured materials is of fundamental interest for developing of quantum information processing systems.

Quantum coherence corrections to conductivity of weakly disordered materials are usually observed as a negative magnetoresistance (positive magnetoconductivity): the quantum interference of electron wave functions, which is known as a weak localization of electrons, determines the magnetoresistance in weak magnetic fields. In fact, even a weak magnetic field B can cause a noticeable phase difference between the two complementary partial-wave amplitudes involved in coherent backscattering, destroying the weak localization regime, then making it visible. The theories of weak localization were first developed in the limit of weak disorder, when the mean free path of electron (l) is much larger than the Fermi wavelength (k_F): $k_F l \gg 1$. In the presence of strong localization or in the variable-range hopping regime, the negative magnetoresistance associated with the quantum interference effects was observed in highly disordered films[8−10] and in compensated GaAs.[11]

In this letter, we present (magneto-) transport measurements of individual In_2O_3 nanowires. The magnetoresistance data have been found to provide quantitative information of electron dephasing mechanisms in these samples. We have observed that the presence of a weak disorder (Anderson-like[12]) arising from doping and electron−boundary collisions leads to a weak localization of electrons as revealed by the positive magnetoconductivity in a large range of temperatures. From the temperature-dependent resistance and magnetoconductivity data obtained in these nanowires, we observed one-dimensional quantum interference effects with electron−electron interaction as the dominant scattering mechanism (leading to the break of the quantum coherence effects). Additionally, the magnetic data provide us with the

* Corresponding author. E-mail: chiquito@df.ufscar.br.
† Departamento de Física, Universidade Federal de São Carlos.
‡ Laboratório Interdisciplinar de Eletroquímica e Cerâmicas, Departamento de Química, Universidade Federal de São Carlos.

10.1021/nl070178k CCC: $37.00
Published on Web 04/19/2007

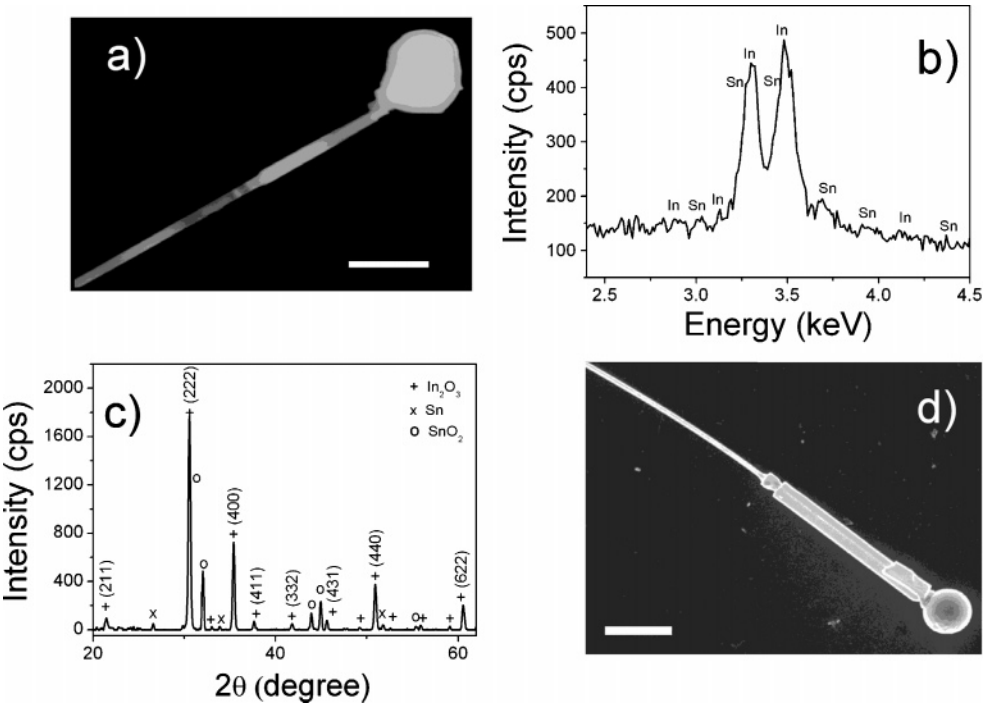

Figure 1. (a) STEM image of a ITO nanowire in bright field mode, and the scale bar is 200 nm; (b) EDS spectrum of a nanowire evidencing the presence of In and Sn is showed. The posterior WDS analysis gives 18.73% atoms of Sn and 81.27% atoms of In. (c) X-ray analysis of the nanowire. The data for In_2O_3 was analyzed following the PDF 6-416 card, and (d) FE-SEM image of a nanowire (the scale bar is 2 μm).

quantitative temperature dependence of the electron dephasing time in the samples. From these results, ITO nanowires become attractive for development of quantum information devices because the coherent transport of electrons was observed until 77 K. To the best of our knowledge, these are the first results on transport parameters like coherent transport in ITO nanowires where $\sigma(B)$ and $R(T)$ were found in agreement with weak localization theories.

ITO nanowires were grown by carbothermal evaporation process of In_2O_3 and SnO_2 powders in a horizontal tube furnace.[13] SnO_2 and In_2O_3 powders (purity >99.9%) were mixed with 10% in weight of carbon black, and each powder was placed inside of two separate alumina crucibles, respectively. The crucibles were placed aligned in the hot zone of a tube furnace with controlled temperature and gas flux. The syntheses were carried out at 1150 °C under a N_2 gas flux of 80 sccm for 6 h. The resulting material, which was collected from the coolest area (extremity) of the tube, had a woolly appearance. The morphology of the nanowires extracted from this material was studied by scanning transmission electron microscopy (STEM) in bright-field mode and by field-emission scanning electron microscopy (FE-SEM), shown in parts a and d of Figure 1, respectively (Zeiss, model Supra 35). The crystal structure of the bulk material was investigated by X-ray diffraction (Rigaku diffractometer), and Miller indices are indicated on each diffraction peak in Figure 1c for the In_2O_3 structure (PDF 6-416). The other peaks are related to Sn metallic and SnO_2, which are present in the self-catalytic vapor−liquid−solid growth mechanism (VLS).[14] The chemical characterization of several nanowires was made using an energy dispersive X-ray spectrometer (EDS, Oxford) attached to a scanning electron microscope (Zeiss, model DSM940A), confirming the presence of In and Sn (Figure 1b). By using a wavelength-dispersive X-ray spectrometer (WDS) also attached to the SEM, the relation of In:Sn obtained was accurately measured, giving 81.27:18.73 atomic. From Figure 1a,d, a droplet was observed in the extremity of the nanowire with high Sn concentration (extracted out by EDS analysis), confirming the VLS mechanism.

Microfabricated metal (Au/Ni, 100 nm) electrodes were prepared onto a thermally oxidized Si wafer with an oxide layer (SiO_2) of 300 nm thickness. Then, the samples were ultrasonically dispersed in ethanol and were placed onto the metallic electrodes. The transport measurements were carried out at different temperatures from 8 to 300 K (±0.1 K) using a closed-cycle helium cryostat and at a pressure lower than 5×10^{-6} Torr. Both the magnetoresistance and resistivity were obtained using standard low-frequency ac lock-in techniques ($f = 13$ Hz). dc measurements were also used, but the results remain unchanged. The measurements were taken in increasing and decreasing B and for $\pm B$, and no hysteresis was observed. We tested different values for the current used in the experiments in order to avoid nonlinear transport due to high field effects. Figure 2 shows a field-emission scanning electron microscopy (FESEM, Zeiss Supra 35, at 5 kV) image of the device used for the measurements. The lateral dimensions of the nanowires shownd in Figure 2 were used for comparison purposes with the characteristic lengths obtained from electrical experiments (the side depletion at the sample's electron density level is negligible).

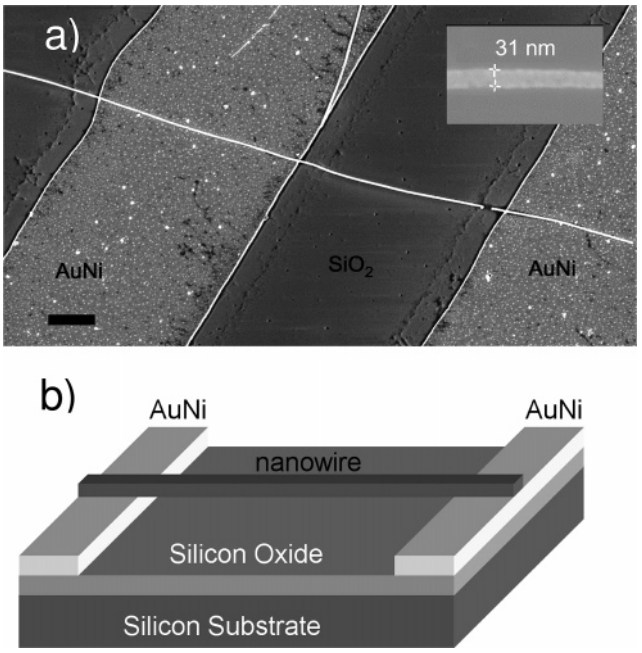

Figure 2. Microfabricated device for measuring individual nanobelts is shown in panel (a). The scale bar is 1 μm. A 31 nm thick Sn doped In_2O_3 nanowire was trapped on the two Au/Ni electrodes of the device (insert). The doping level used was $n = 1.8 \times 10^{20}$ cm^{-3}. (b) Sketch of the device.

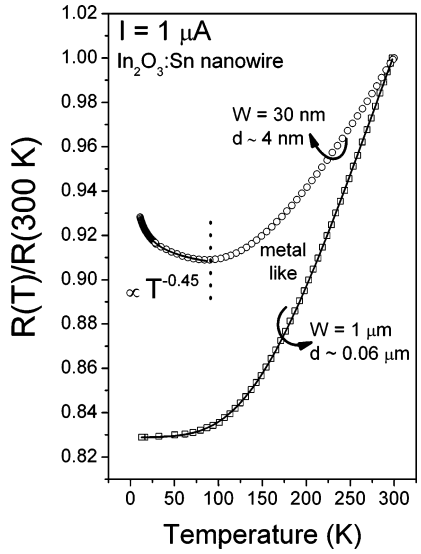

Figure 3. Temperature-dependent resistance measurements for two different samples. Note that the saturation of the metallic character (solid line is the theoretical fit), presented by the larger sample, was not observed for the smaller one, which in turn shows a localized behavior for $T < 77$ K. The solid line (10−77 K, smaller sample) is the theoretical fit to the power law $R(T) = R_0 + R_1T^{-n}$, yielding $n = 0.458$. This sample was characterized by low electron mobility (~20 cm^2/Vs, calculated from the resistance−temperature data).

The temperature-dependent resistance data ($B = 0$) are plotted in Figure 3. The larger sample exhibits a metallic behavior for the whole temperature range used in the experiments and saturates below 77 K. This behavior agrees very well with the Bloch−Grüneisen theory for the dependence of the electrical resistance on the electron-acoustic phonon scattering mechanism. In this way, the resistance is described by[15]

$$R(T) = R_0 + A\left(\frac{T}{\Theta_D}\right)^n \int_0^{\frac{\Theta_D}{T}} \frac{z^n e^z}{(e^z - 1)^2}\,dz \qquad (1)$$

where A and R_0 are constants and n usually ranges from 3 to 5 when the electron−phonon interaction is mainly responsible for the scattering events;[15−16] Θ_D is the Debye temperature. The fitting of the experimental data using eq 1 revealed $n = 3.7$ and $\Theta_D = 1153$ K: as the temperature and phonon excitation increase, the amount of scattering events experienced by the conduction electrons are increased as well, resulting in a greater resistance.

On the other hand, the smaller sample shows two distinct characteristics for the electron transport. A localized character (from 8 to ~77 K) and a metallic one from ~77 to 300 K (increase of the resistance with increasing temperature, $n = 3.6$ and $\Theta_D = 1210$ K, not shown) were observed in the samples. Because the ITO nanowires are expected to remain metallic, the carrier density is a weak function of temperature and the resistance should be mainly determined by the temperature dependence of the various scattering mechanisms. At high temperatures ($T > 77$ K), the phonon scattering seems to be dominant and the resistance rises with increasing temperature (metallic phase), in agreement with the behavior presented by the larger sample. As the temperature is lowered, other scattering mechanisms become dominant, giving rise to a distinct temperature-dependent resistance for $T < 77$ K, which explains in part the general features of the curve presented in Figure 3 (smaller sample).

The scattering mechanism at low temperatures can be related with the size of the samples: as the nanowire cross section decreases, the boundary scattering becomes relatively more important than for larger wires because a larger portion of the carriers are located near the wire boundary. Then (1) for small-dimension nanowires, the disorder coming from processes like collisions with the boundaries[17−18] provides the necessary disorder to randomize electron energy, resulting in a localized character for the transport; (2) this will increase the electron−electron interaction as well.[19] It is important to emphasize that the increase of the resistance below 77 K is not related with strong localization: the disorder from boundary scattering, randomizing the electron potential, is not enough to promote strong localization. In fact, successive attempts in order to distinguish an activation law, $R \propto \exp(E/k_BT)$ or a variable range hopping, $R \propto \exp(T_0/T)^{1/2}$ behavior have failed.

The solid line presented in Figure 3 for $T < 77$ K (smaller sample) was the best fit of the experimental data to the dependence $R(T) = R_0 + R_1T^{-n}$, yielding $n = 0.458$. This is in close agreement with that expected for one-dimensional electron−electron interactions,[20] and this mechanism should be addressed as the dominant scattering source at low temperatures (as a consequence, it is the source of the electron dephasing).

To shed light on this issue, we performed magnetoconductivity measurements. As is well-known, weak disorder

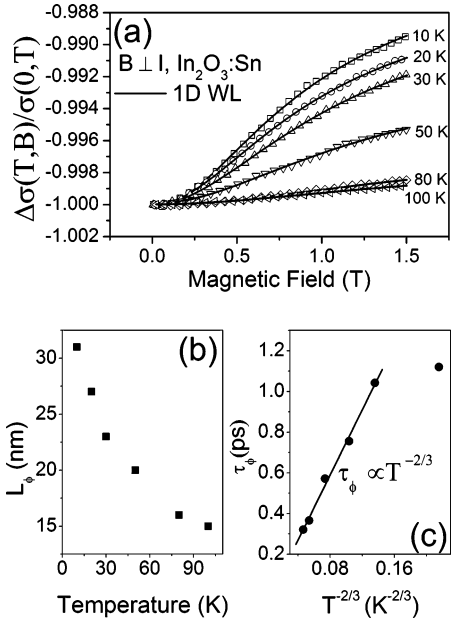

Figure 4. Magnetoconductivity data for 10 K < T < 77 K is shown in panel (a). The theoretical lines fit well the experimental data, as shown by the solid lines. These lines correspond to the one-dimensional weak localization (1D WL) correction to the conductivity. From the fitting procedure, we found the coherence length L_ϕ and the phase breaking time τ_ϕ, plotted in panels (b) and (c) as a function of the temperature, respectively.

leads to a weak localization due to constructive quantum interference of time-reversed electron trajectories.[20] At T < 77 K, the character of the transport in our samples should be controlled by quantum interference effects, which in turn should be observed in the magnetoconductivity of the narrower nanowire. Figure 4a shows the magnetoconductivity data obtained at different temperatures, using the usual $B \perp I$ geometry ($I = 1\ \mu$A), with the magnetic field B ranging from 0 to 1.5 T. The presence of the electron quantum interference effects was then readily observed: the increase of the conductivity with increasing magnetic field over the whole temperature range used for the experiments.

The experimental data was analyzed using the 1D localization correction to the conductivity in a system with little or no spin−orbit scattering[19−22] given by

$$\Delta\sigma(B) = \frac{2e^2}{Lh}\left[\frac{1}{L_\phi^2} + \frac{1}{D\tau_B}\right]^{-1/2} \qquad (2)$$

where

$$\tau_B = \frac{3}{4}\frac{L_B^4}{W^2 D} \text{ and } L_\phi = \sqrt{D\tau_\phi} \qquad (3)$$

Here, L_ϕ is the coherence length (distance in which electrons can travel coherently without phase lost) D is the diffusion coefficient (7×10^{-4} m^2 s^{-1}), and τ_ϕ is the phase breaking time; $L_B = (\hbar/eB)^{1/2}$ is the magnetic length; W and L are the width and length of the channel conducting electrons. It should be noted that L_ϕ is directly obtained from the fitting of the experimental data to eq 2. To be one-dimensional with respect to the quantum interference effects, a conductor should have cross-sectional dimensions of the order of the coherence length of the electron wave function. In fact, the phase coherence length L_ϕ decreases from 31 nm at 10 K to 15 nm at 100 K as plotted in Figure 4b: the high-temperature fit becomes worse and the precision in estimating of L_ϕ decreases (the increase of inelastic phonon scattering progressively breaks the weak localization).

Figure 4c shows the variation of the phase breaking time on the temperature. The experimental data were well fitted by using the dependence

$$\tau_\phi = \left(\frac{e2\sqrt{2D}k_B R}{\hbar^2 L}T\right)^{-2/3} \qquad (4)$$

expected for 1D systems.[23] Here, R/L is the resistance of a 1D sample per unit length. This provides additional evidence that electron−electron interactions are the source of the one-dimensional inelastic scattering causing the coherent transport breaking, as shown by the experimental data. The prefactor in eq 4 was found to be 7.6 ps, while theoretical calculations give 0.9 ps. Taking into account that we have not used adjustable parameters for the fit, the agreement between both experimental and theoretical values is quite remarkable. The difference could be eventually due to an underestimation of the diffusion constant and due to uncertainties in the effective length of the sample.

It should be noted that the results from temperature- and magnetic field-dependent quantities characterizing the dimensionality of the scattering processes and the contribution of the electron−electron interaction to the resistance are in agreement. Both of these processes should be controlled by the same thermal scale length, $L_T = (D\hbar/k_B T)^{1/2} \sim 25$ nm (10 K), which is close to $L_\phi = 31$ nm (which determines the dimensionality of the sample with respect to quantum interference effects) and to the width of the sample, $W = 31$ nm, confirming in turn the one-dimensional character of the sample.

Electronic properties of self-assembled high crystalline quality tin-doped indium oxide were studied. We report the experimental data and the related analysis on the resistance and magnetoconductivity of these single-crystal nanowires. The temperature dependence of the electrical resistance was studied from 10 to 300 K, and different conduction mechanisms were observed: for T > 77 K, the resistance follows the Bloch law for metallic systems, and at low temperatures, the resistance was found to be controlled by the electron−electron scattering. Additionally, transport parameters like coherence length and dephasing time were found in agreement with 1D weak localization theories. Our result suggests that, by decreasing the dimensions of the wires, it would not be possible to retain the metallic characteristic of the transport without degradation of the electronic properties of the devices (due to quantum effects), as evidenced by the change from metallic to a nonmetallic character of the transport. Moreover, the samples show features of coherent

transport of electrons that persist until high temperatures, making them attractive for further investigations aimed at development of novel devices.

Acknowledgment. We thank the Brazilian research funding Agencies FAPESP and CNPq for the financial support of this work. We are indebted to R. C. Motta and J. Alves Pinto for technical assistance.

References

(1) Prinz, G. A. *Science* **1998**, *282*, 1660.
(2) Postma, H. W. C.; Sellmeijer, A.; Dekker, C. *Adv. Mater.* **2000**, *17*, 1299.
(3) Baughman, R. H.; Zakhidov, A. A.; de Heer, W. A. *Science* **2002**, *297*, 787.
(4) Ronning, C.; Gao, P. X.; Ding, Y.; Wang, Z. L.; Schwem, D. *Appl. Phys. Lett.* **2004**, *84*, 783.
(5) Datta, S. *Electronic Transport in Mesoscopic Systems*; Cambridge University Press: Cambridge, U.K., 1997.
(6) Landauer, R. *IBM J. Res. Dev.* **1957**, *1*, 223.
(7) Heremans, J.; Thrush, C. M.; Zhang, Z.; Sun, X.; Dresselhaus, M. S.; Ying, J. Y.; Morelli, D. T. *Phys. Rev. B* **1998**, *58*, 10091.
(8) Sivan, U.; Entin-Wohlman, O.; Imry, Y. *Phys. Rev. Lett.* **1988**, *60*, 1566.
(9) Farah, O.; Ovadyahu, Z. *Phys. Rev. B* **1988**, *38*, 5457.
(10) Ovadyahu, Z. *Phys. Rev. Lett.* **1984**, *52*, 569.
(11) Benzaquen, M.; Walsh, D.; Mazuruk, K. *Phys. Rev. B* **1988**, *38*, 10933.
(12) Anderson, P. W. *Phys. Rev.* **1958**, *109*, 1492.
(13) Leite, E. R.; Gomes, J. W.; Oliveira, M. M.; Lee, E. J. H.; Longo, E.; Varela, J. A.; Paskocimas, C. A.; Boschi, T. M.; Lanciotti, F., Jr.; Pizani, P. S.; Soares, P. C., Jr. *J. Nanosci. Nanotechnol.* **2002**, *2*, 125.
(14) Chen, Y. Q.; Jiang, J.; Wang, B.; Hou, J. G. *J. Phys. D: Appl. Phys.* **2004**, *37*, 3319.
(15) Ziman, J. M. *Electrons and Phonons*; Claredon Press: Oxford, 1960.
(16) Al'tshuler, B. L.; Aronov, A. G. *Electron−Electron Interaction in Disordered Conductors*; Efros, A. L., Pollak, M., Eds.; North Holland: Amsterdam, 1985.
(17) Thornton, T. J.; Roukes, M. L.; Scherer, A.; Van der Gaag, B. P. *Granular Nanoelectronics*; Ferry, D. K., Baker, J. R., Jacoboni, C., Eds.; NATO ASI Series; Plenum Press: New York, 1991.
(18) In_2O_3 and other oxide-based nanowires are known to present a large affinity with chemical species like O_2 molecules that can be adsorbed on the nanowire surface and react with the nearby free electrons in order to form a superficial O_2^- layer. To verify this, we have conducted experiments using ultraviolet light, but the resistivity−temperature curves were not changed. Besides that, even in the presence of a low density of O_2 adsorbed molecules, the electron potential nearby the surface should be randomized.
(19) Lin, J. J.; Bird, J. P. *J. Phys. Condens. Matter* **2002**, *14*, R501.
(20) Beutler, D. E.; Giordano, N. *Phys. Rev. B* **1988**, *38*, 8.
(21) Heremans, J.; Thrush, C. M.; Yu-Ming L.; Cronin, S. B.; Dresselhaus, M. S. *Phys. Rev. B* **2001**, *63*, 085406.
(22) Schönenberger, C.; Bachtold, A.; Strunk, C.; Salvetat, J.-P.; Forró, L. *Appl. Phys. A* **1999**, *69*, 283.
(23) Gershenson, M. E. *Ann. Phys.* **1999**, *8*, 559.

NL070178K